Geosciences and Engineering, Vol. 8, No. 13 (2020), pp. 45–69.

HEAT FLOW DENSITY DETERMINATIONS IN HUNGARY USING WELL LOGS

JÁNOS MIHÁLYKA[1*] – PETRA PARÓCZI[1] – LÁSZLÓ LENKEY[1]

[1]*Department of Geophysics and Space Sciences, Eötvös Loránd University*
mihalyka.janos@ttk.elte.hu

Abstract: The thermal conductivity of rocks can be deduced from available data of exploration wells such as core samples, cuttings, lithological descriptions and geophysical well logs. As the thermal conductivity of clastic sediments is lower than the conductivity of the crystalline basement, the sediments have a significant influence on the temperature distribution and heat flow density. We present a methodology for determining the thermal conductivity of clastic sediments using geophysical well logs and thermal conductivity data measured in laboratory. Our results are based on the data of 6 exploration wells. Several well log combinations and thermal conductivity measurements from 70 core samples were used to work out the method. The lithological composition consisting of shale, sand and water was identified and the volumetric fractions of these components were derived from wireline logging data such as natural gamma ray, resistivity, bulk density and neutron porosity logs. The lithological composition was determined with Bayesian inversion applying the weighted least squares method. The effective thermal conductivity was computed by applying an appropriate mixing law using the thermal conductivity values of the lithological components. The thermal conductivities derived from well logs were tested and new matrix thermal conductivity values were calculated using archive thermal conductivity measurements of core samples. The harmonic mean model proved to be the best mixing law, resulting in the best fit to laboratory measurements. The reliability of our model was also tested with the help of temperature measurements carried out in a well. Heat flow density determinations were carried out using the Bullard-plot technique with thermal conductivities calculated by our new method. In case of 6 wells, heat flow densities calculated by the new method are in the range of heat flow density values previously conducted but with substantially lower uncertainties.

Keywords: *thermal conductivity, mixing models, heat flow density, well log interpretation, geophysical inversion*

1. INTRODUCTION

The utilization of geothermal energy in Hungary has a long tradition, because several geothermal reservoirs exist in the Tertiary and Quaternary sediments and buried karstified and fractured carbonates. Almost 70% of Hungary's surface is covered by Tertiary and Quaternary clastic sediments. The average sediment thickness is 1–2 km, but in the deepest troughs it reaches 5–8 km *(Figure 1)*. As the thermal conductivity of clastic sediments is lower than the conductivity of the crystalline basement, the sediments have a significant influence on the temperature distribution and heat

flow density. The heat flow density is one of the most important quantities in geothermal exploration, because it allows the prediction of subsurface temperature, and its local variations may originate from groundwater flow, which indicates the presence of a reservoir [1–3]. Its large scale distribution is also influenced by mantle and lithospheric processes, therefore it is an important control parameter in geodynamic models [4–5]. The heat flow density is determined using Fourier's Law as the product of the thermal conductivity of rocks and the temperature gradient measured in boreholes and wells.

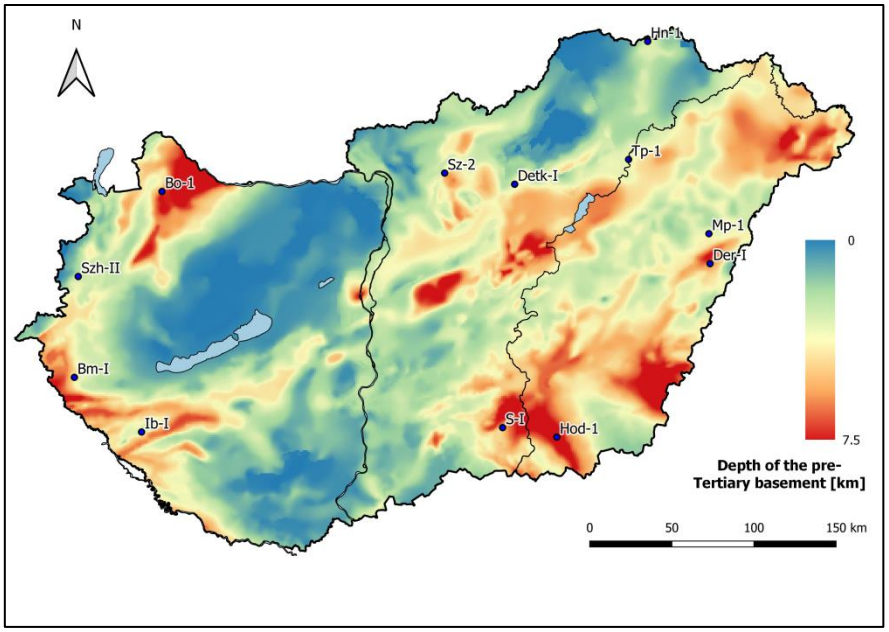

Figure 1
The locations of the drilling projects in Hungary. The color scale represents the depth of the pre-Tertiary basement (after Kilényi et al. [6]*)*

Detailed thermal conductivity data are required to separate the conductive and convective heat flow density, for instance, in numerical models. It is impossible to acquire thermal conductivity data with such resolution from laboratory measurements alone. Coring processes to obtain core samples are expensive techniques to reach a good spatial and depth resolution. Additionally, core samples can get damaged during their transportation and laboratory measurement. However, well log data offer good resolution, and thus one of the main goals of this study is to develop a method to determine thermal conductivity of the Tertiary and Quaternary clastic sediments using well logs.

One of the basic ways to establish a relationship between the thermal conductivity and well logs is to compute the lithological composition, usually consisting of shale, sand, marl and water, using openhole logging measurements (natural gamma ray,

density, neutron porosity, resistivity etc.) and then apply an appropriate mixing law amongst the components to obtain the thermal conductivity [7–10]. The mixture models describing the thermal conductivity of a rock can be grouped into (1) well-defined physical models (Hashin and Shtrikman bounds) and (2) purely empirical or semi-empirical approaches (geometric, arithmetic or harmonic mean) [11].

The behavior of different mixing models in case of sedimentary rocks was analyzed by several authors. In the work of Hutt & Berg [12] bulk thermal conductivities calculated by several mixing models (arithmetic mean, harmonic mean, geometric mean) were compared to values measured with a needle probe on 28 sandstone samples. The harmonic mean showed a good fit, whereas the arithmetic and geometric mean models overestimated the measured data. Brigaud et al. [7] mentioned the fact that the properties of certain lithotypes containing clay can change during drilling, causing systematic errors. In their work, the geometric mean model was identified as a suitable method to calculate the bulk thermal conductivity. Hartmann et al. [9] also concluded that the geometric mean mixing law can be a reliable choice in case of argillaceous and marly lithology. Fuchs et al. [11] provided a validity study of simple and generally used mixing models for a two-phase rock system based on the work of Clauser [13], which in turn was based on 1,147 laboratory measurements conducted on sandstone, mudstone, limestone and dolomite samples with the optical scanning method [14]. The geometric mean model seemed to be the best choice with a poor coefficient of determination ($R^2 = 0.62$), thus they developed correction charts to increase the R^2 values of mixing models.

Drillings — where well-log data and thermal conductivity measurements are available — are needed to successfully elaborate the method. There are 12 exploration wells in Hungary where these measurements are accessible *(Figure 1)*, and the whole dataset of 6 drillings labeled Bo-1, Szh-II, S-I, Der-1, Mp-1, Sz-2 have been successfully collected, quality controlled and digitized. In the listed wells the following log types were available: spontaneous potential, natural gamma ray, resistivity, neutron porosity and bulk density logs.

The thermal conductivity measurements on core samples were carried out with the Transient Line Source method [15] based on the work of Cull [16]. The average relative error of this measurement technique is 10–15% according to measurements performed on standard samples [15]. 70 core samples were used in the elaboration, and in most cases two or three measurements were made on the samples, thus altogether 158 thermal conductivity measurements were taken into account. Regarding the rock types, 38 core samples fell into the group of pelites (clay, silt and marl) and 32 core samples represented the group of psammites (sand, sandstones). The fluid content was preserved by waxing the samples.

Our main goal was to elaborate a methodology for determining the thermal conductivity of clastic sediments using geophysical well logs and to calculate the heat flow density in a quality-controlled way. Thus, improving the method of the determination of the thermal conductivity significantly increases the precision of the heat flow density calculation and can increase the reliability of thermal models.

2. METHODOLOGY

2.1. Well log analysis

A geophysical inversion algorithm based on a weighted least squares method was developed using the Mathcad software. The main goal of the inversion is to derive the volumetric fractions (p_i) of the lithological components from wireline logging data such as natural gamma ray, resistivity, compensated bulk density and neutron porosity measurements. The lithological composition — determined with Bayesian inversion — is assumed to be a mixture of clay (cl), sandstone (ss), and water (w). The conventional inversion is based on maximum likelihood principle and the measurement noise is assumed to be additive centered Gaussian noise. In the case presented, the sum of squares of the differences between the measured and the recalculated data is minimized to evaluate the best fitting parameter vector of the volumetric fractions. The correction for the input parameter vector of the inversion ($\Delta\mathbf{p}$) can be calculated as follows [17]:

$$\Delta\mathbf{p} = \mathbf{R}^{-1}\mathbf{F}^{T}\mathbf{W}\Delta\mathbf{y}, \tag{1}$$

where **F** is the Jacobi's matrix, **W** is the weighting matrix, $\Delta\mathbf{y}$ is the difference vector between the observed and the calculated data, and **R** is the so-called iteration matrix, described as

$$\mathbf{R} = \mathbf{F}^{T}\mathbf{W}\mathbf{F}. \tag{2}$$

The probe response equations can be seen in *Table 1*.

Table 1

Petrophysical descriptors

Petrophysical descriptor	**Unit**	**Equation**
Natural gamma ray	μR/h	$GR(\mathbf{p}) = p_1\gamma_1 + p_2\gamma_2 + (1-p_1-p_2)\gamma_3$
Bulk density	g/cm^{-3}	$\rho_b(\mathbf{p}) = p_1\rho_1 + p_2\rho_2 + (1-p_1-p_2)\rho_3$
Neutron porosity	v/v	$\Phi_N(\mathbf{p}) = p_1\Phi_{N_1} + p_2\Phi_{N_2} + (1-p_1-p_2)\Phi_{N_3}$
Resistivity	ohmm	$R_t(\mathbf{p}) = \dfrac{4\cdot(1-p_1-p_2)^m}{a\cdot R_w\cdot\left[\left(\dfrac{S_w\cdot 2\cdot(1-p_1-p_2)^m}{a\cdot R_w}+\dfrac{p_1}{R_{cl}}\right)^2-\dfrac{p_1}{R_{cl}}\right]}$

Nomenclature:

p_1	Volume fraction of clay	Φ_{N1}	Neutron-porosity of clay
p_2	Volume fraction of sand	Φ_{N2}	Neutron-porosity of sand
γ_1	Natural gamma ray of clay	Φ_{N3}	Neutron-porosity of water
γ_2	Natural gamma ray of sand	R_{cl}	Resistivity of clay
γ_3	Natural gamma ray of water	R_w	Resistivity of water
ρ_1	Bulk density of clay	S_w	Water saturation
ρ_2	Bulk density of sand	a	Tortuosity factor
ρ_3	Bulk density of water	m	Cementation exponent

The measured data is often characterized by different degrees of uncertainty. In order to take this effect into consideration, a given weight proportional to the uncertainties is contributed to the solution. The applied weighting matrix is symmetric and its diagonal elements are the reciprocal of squares of the particular measurement's standard deviations, which were determined by the sample standard deviation formula along a clear lithological zone.

To examine the statistical features of the estimated parameters, their covariance matrix has been determined in each depth point which includes the squares of the parameters' standard deviation values in its main diagonal:

$$\sigma_i = \sqrt{\mathbf{C}_{i,i}}, \tag{3}$$

where σ_i is the standard deviation of the *i*th parameter and **C** is the covariance matrix of the calculated model parameters in a given depth point.

2.2. Mixing models

Several mixing models were applied in this work. These are the four most frequently used models: arithmetic, geometric, harmonic means and the Hashin-Shtrikman bounds. Calculating the bulk thermal conductivity (λ_b) of a two-component rock system involves the thermal conductivity of the matrix (λ_m), the effective porosity (Φ), and the thermal conductivity of the pore content (λ_p). Using the sensitive relationship between porosity and bulk thermal conductivity is the root of every mixing model: the thermal conductivity of the pore fluid is fairly low regarding the matrix thermal conductivity. Porosity and the volumetric fraction of matrix can be derived from geophysical well logs.

2.2.1. Arithmetic and harmonic mean

Frequently used approaches are the arithmetic and harmonic mean, both of which are based on a layered model where the thermal conductivity depends on the direction of the heat flow density. If the heat flow is parallel to the layering, the bulk thermal conductivity is equal to the arithmetic mean of the lithological components (matrix and pore content) weighted by their volumetric fractions [11]:

$$\lambda_b = (1-\phi)\cdot\lambda_m + \phi\cdot\lambda_p. \tag{4}$$

Assuming heat flow density perpendicular to the layering, the harmonic mean can be used to calculate the bulk thermal conductivity:

$$\lambda_b = \frac{1}{\frac{1-\phi}{\lambda_m} + \frac{\phi}{\lambda_p}}. \tag{5}$$

According to Voigt [18] and Reuss [19], these mixing models can be defined as the upper (arithmetic) and lower (harmonic) bounds of the thermal conductivity.

2.2.2. Hashin–Shtrikman bounds

Narrower bounds can be derived by the theory of Hashin and Shtrikman [20]. The upper bound represents a geometry assuming fluid-filled, spherical pores in a solid rock matrix:

$$\lambda_{HS}^{U} = \lambda_m + \frac{\phi}{\frac{1}{(\lambda_p - \lambda_m)} + \frac{(1-\phi)}{3\lambda_m}}. \tag{6}$$

The lower bound can be derived by assuming a geometry where the solid fraction is represented as spherical grains suspended in a fluid:

$$\lambda_{HS}^{L} = \lambda_p + \frac{(1-\phi)}{\frac{1}{(\lambda_m - \lambda_p)} + \frac{\phi}{3\lambda_p}}. \tag{7}$$

Theoretically, the thermal conductivities of rock samples should fall in between these bounds.

2.2.3. Geometric mean

The geometric mean model is the most popular approach. It is a pure empirical formula providing a simple mathematical expression to calculate the bulk thermal conductivity (see e.g. [11]):

$$\lambda_b = \lambda_m^{1-\phi} \cdot \lambda_p^{\phi}. \tag{8}$$

2.2.4. Thermal conductivity of lithological components

The most critical part of calculating the bulk thermal conductivity is choosing an appropriate mixing law and using correct thermal conductivity values for the given components. In this work, a three-component lithological model was utilized, which means a mixture of clay, sandstone and water as pore fluid. The thermal conductivity of the sandstone and clay parameter was chosen after the work of Dövényi & Horváth [21]. The Tertiary and Quaternary sediments of the Pannonian Basin can be divided in two broad lithological categories: pelites (including clay, claystone and marl) and psammites (including sand, sandstone and gravel). This classification was implemented on core samples used in Dövényi & Horváth's laboratory measurements [21]. They established thermal conductivity – depth functions and calculated the matrix thermal conductivity of pelites and psammites using the geometric mean with porosity values derived from the national porosity trend of Hungary *(Figure 2)*. Thus, in the first step, the conductivity of the sandstone (psammites) and clay parameter (pelites) was set to 4.2 and 2.8 W/(m*K), respectively.

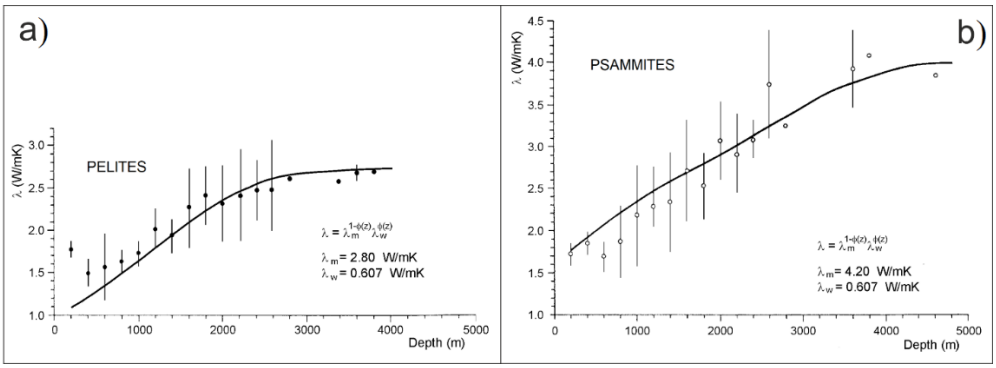

Figure 2

Thermal conductivity vs. depth functions of pelites (a) and psammites (b) based on laboratory Transient Line Source measurements (Dövényi & Horváth [21]*)*

2.3. Heat flow density

The final step of the methodology is calculating the heat flow density. It can be determined by Fourier's law: the product of thermal conductivity and temperature gradient.

2.3.1. Bullard plot

Other methods are also available for calculating the heat flow density. For our dataset, the Bullard-plot technique was the most suitable method for the heat flow density determination. Assuming an isotropic, horizontally layered medium where the heat flows only in vertical direction, the following equation can be used:

$$T_i = T_0 + q\sum_{j=1}^{i}\frac{\Delta z_j}{\lambda_j}, \tag{9}$$

where T_i [°C] is the measured temperature in the ith depth, T_0 [°C] is the surface temperature, q [mW/m^2] is the heat flow density. The summation — to the ith depth of the quotient of the depth interval (Δz_j) and the thermal conductivity [W/(m*K)] derived from our methodology — is called thermal resistance. Plotting the measured temperatures as a function of thermal resistance, a linear fitting can be applied to the data. The slope of the linear fit will describe the heat flow density *(Figure 3)*.

It is important to take into consideration the temperature and pressure dependence of thermal conductivity. Increasing temperature will have a negative effect on the thermal conductivity; on the other hand, increasing pressure with depth will lead to higher thermal conductivity. For temperature correction, we used Sommerton's formula [22]:

$$\lambda_T = \lambda_{20} - 10^{-3}\cdot(T-293)\cdot(\lambda_{20}-1.38)\cdot\left[\lambda_{20}\cdot(1.8\cdot10^{-3}\cdot T)^{-0.25\cdot\lambda_{20}} + 1.28\right]\cdot\lambda_{20}^{-0.64}, \tag{10}$$

where T [°C] is the temperature and λ_{20} [W/(m*K)] is the measured thermal conductivity at room temperature. For pressure correction the formula of Fuchs & Förster [10] was applied:

$$\lambda_p = (1.095 \cdot \lambda_{lab} - 0.172) \cdot p^{(0.0088 \cdot \lambda_{lab} - 0.0067)}, \tag{11}$$

where p is assumed to be in situ pressure in MPa and λ_{lab} [W/(m*K)] is the thermal conductivity measured at the surface. The first step was applying the temperature correction, then the temperature corrected thermal conductivity was replaced in the formula of the pressure correction as a second step of the correction. Finally, the corrected thermal conductivity values were used in *Equation (9)*.

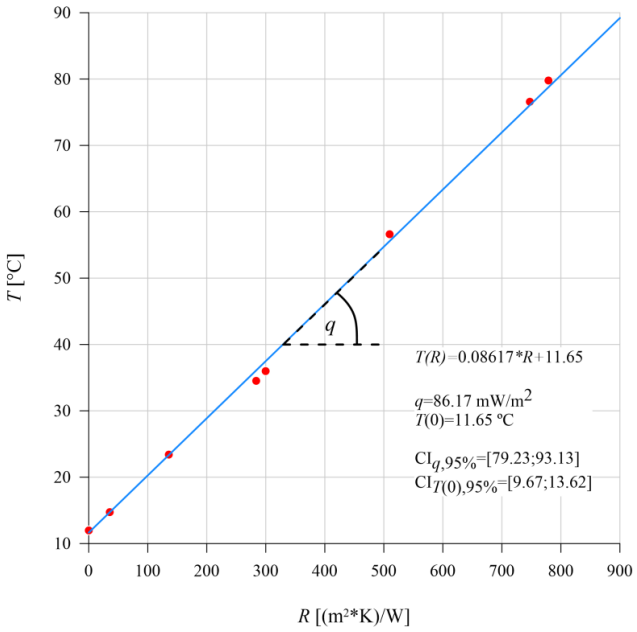

Figure 3

The Bullard plot: linear fit between the temperature (T) and thermal resistance (R). The slope and the intercept of the linear fit give the value of the heat flow density (q) and surface temperature (T(0)), respectively. $CI_{q,95\%}$ and $CI_{T(0),95\%}$ are the 95% confidence intervals of the slope and intercept.

2.3.2. Error propagation

It is important to define the uncertainty of the heat flow density. The Gaussian error propagation formula was applied for this purpose:

$$s_f \approx \sqrt{\left[\sum_i \left(\frac{\partial f}{\partial x_i}\right)^2 \cdot \sigma_{x_i}^2\right] + 2\sum_{i<j}\left[\left(\frac{\partial f}{\partial x_i}\right)\left(\frac{\partial f}{\partial x_j}\right)\mathrm{cov}(x_i, x_j)\right]}, \tag{12}$$

where s_f is the standard deviation of the f function, σ_{xi} is the standard deviation of the parameter x_i and cov is the covariance of the parameters.

The standard deviations and covariances of the clay, sand and water parameters derived from the geophysical inversion were used for calculating the error propagation of the thermal conductivities using *Equation 12*. The effects of the temperature and pressure corrections were also taken into consideration. The final step was to calculate the error propagation of the thermal resistances using the calculated standard deviations of the thermal conductivities.

Applying the Bullard-plot technique, the error propagation of the thermal resistances and the uncertainty of the temperature values were also used as weights for the linear fit after the work of York [23] and York et al. [24] *(Figure 4)*. Subsequently, the standard deviation of the slope of the linear fit was assumed to be the error propagation of the heat flow density.

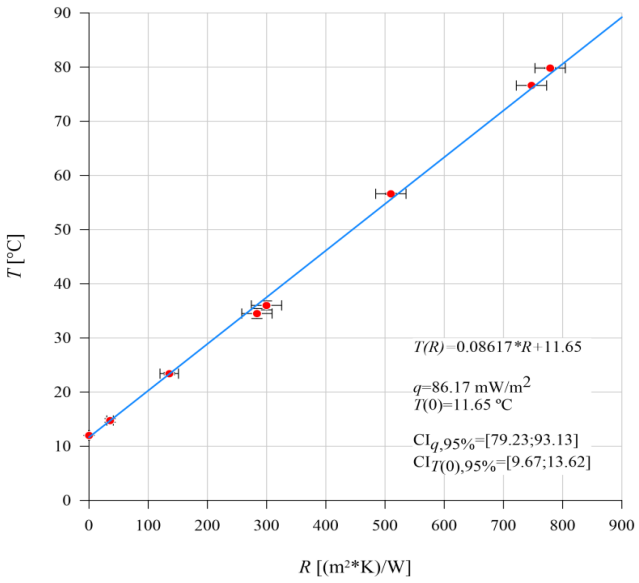

Figure 4

The Bullard plot: weighted linear fit between the temperature (T) and thermal resistance (R). The slope and the intercept of the linear fit give the value of the heat flow density (q) and surface temperature (T(0)), respectively. $CI_{q,95\%}$ and $CI_{T(0),95\%}$ are the 95% confidence intervals of the slope and intercept.

3. RESULTS

3.1. Lithological model

Our main purpose is determining the thermal conductivity of Tertiary and Quaternary clastic sediments in order to build a lithological model that not only represents realistically the sediments filling in the Pannonian Basin but provides a statistically satisfying result after the inversion process.

In a stratigraphy-sedimentology study Juhász [25] synthesized the main lithofacies units common in the Pannonian s.1. sequence of the Neogene subbasins considering the new unified lithostratigraphic nomenclature. On the basin plain basal marls formed beginning with calcareous marl grading into argillaceous marl upwards, which consists of the Endrőd Formation. The Szolnok Sandstone Formation represents the deep-water turbidite sequence of fine-grained sandstones transported from the shelf edge to the deep sea *(Figure 5)*. Afterwards both the delta and basin slope sediments reach huge thicknesses, built up by argillaceous marls and siltstones with sandstone interbeds. This depositional environment contains the Algyő Formation. In the deltaic environments a large amount of littoral sediments deposited, forming a thick, sandy, continuous lithofacies association which comprises the Újfalu Formation *(Figure 5)*. The Zagyva Formation represents fluvial or alluvial sediments concentrated in particular regions with thin lignite beddings in some areas; however, in the northern part of the Pannonian Basin thicker lignite and brown coal beds formed — called the Bükkalja Member — because of the negligible amount of sediment input.

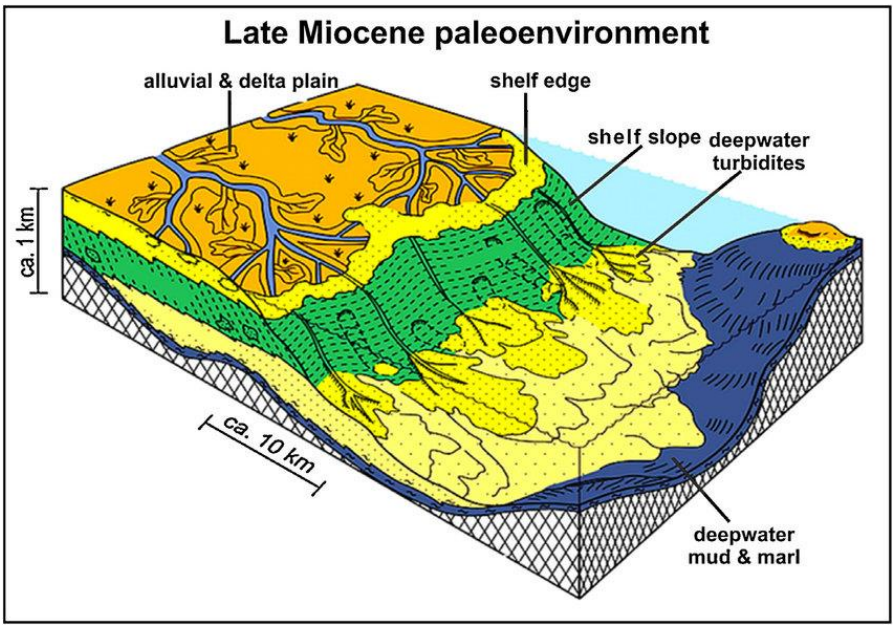

Figure 5
Generalized cross-section of the characteristic depositional environments in the Late Miocene [26]

All of the mentioned formations are penetrated by the examined exploration wells, although some of the drillings reached the Lower Badenian (Middle Miocene) sediments. The Lower Badenian cycle of sedimentation comprises the Hidas Formation forming brown coal beds with argillaceous sand, sandy clay marls and clay

interbeddings. The Szilágy Formation represents a pelagic lithofacies with well layered silty or fine-grained sandy clays, clay marls, and marls. This sedimentary cycle ended with regression in the end of the Badenian, with the Kozárd Formation representing a new period of transgression in the evolution of the basin. The sequence deposited in littoral or even paludal, shallow and deep sublittoral environments is diversified mainly by arenose sands with aleurite bands. The neritic or shelf facial Tinnye Formation seems to laterally interfinger with the Kozárd Formation consisting of layered clay marls with sandstone and aleurit interbeds.

To emphasize the conclusions of the stratigraphy, we summarize the main rocks occurring in this study: sandstone, argillaceous sand, sandy clay, silty clay, clay, clay marl, argillaceous marl, marl, aleurit, lignite and brown coal bands. On the basis of the listed elements, a lithological model assumed to be a mixture of clay, sandstone and water is acceptable.

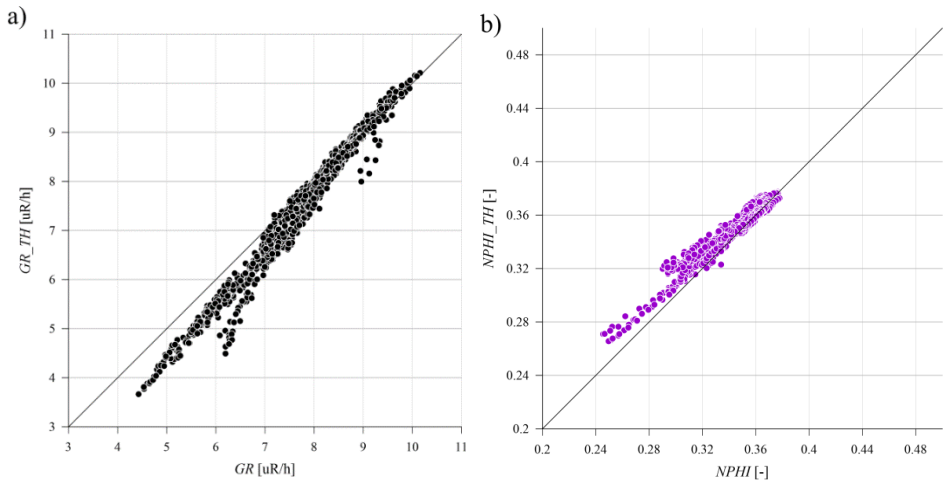

Figure 6

Crossplots of the measured and recalculated logs in case of gamma ray (a) and neutron porosity (b) logs. GR and NPHI indicate the measured data, GR_TH and NPHI_TH mean the recalculated values

Our results confirm the pertinence of this lithological model, which can be verified by the fitting of the recalculated log data and the standard deviations of the estimated parameters. The crossplots in *Figure 6* show a good fit between the measured and recalculated data. Similarly, the example interval presented in *Figure 7* also shows that the recalculated gamma ray, bulk density, neutron porosity and resistivity log fitting satisfyingly well to the original measured data. The model was also confirmed by examining the average standard deviation values of clay, sandstone, and water fractions which are 5.4%, 4.8% and 2.7%, respectively. Nevertheless, there are depth sections where the inversion is uncertain, probably due to the poor quality of measurement techniques, but fortunately the core sampling intervals are not affected.

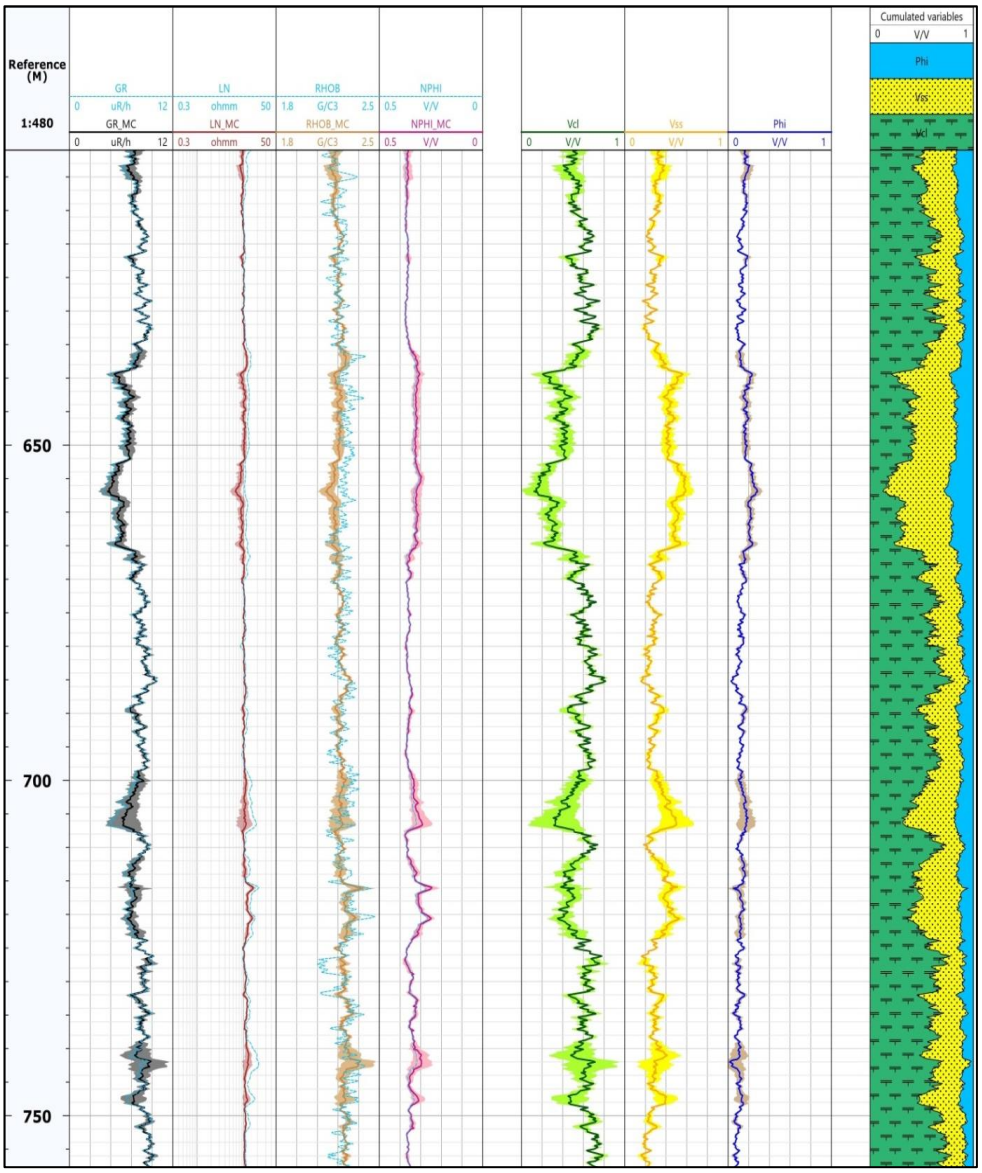

Figure 7

Results of the inversion from the Sz-2 well consisting of Lower Pannonian (Late Miocene) sediments. Input curves are light blue and dash lined, recalculated curves: black: natural gamma ray, red: resistivity, orange: bulk density, pink: neutron porosity, result curves: green: volume fraction of clay, yellow: volume fraction of sandstone, purple: porosity filled with water. The shaded areas define the standard deviations of each variable. Last column represents the lithological model: green: volume fraction of clay, yellow: volume fraction of sandstone, blue: pore water.

3.2. Thermal conductivity

3.2.1. Thermal conductivities calculated using matrix thermal conductivities after the work of Dövényi & Horváth [21]

The bulk thermal conductivities — calculated by using different mixing models — were compared to laboratory measurements conducted on core samples, thus several thermal conductivity logs were created *(Figure 8)*.

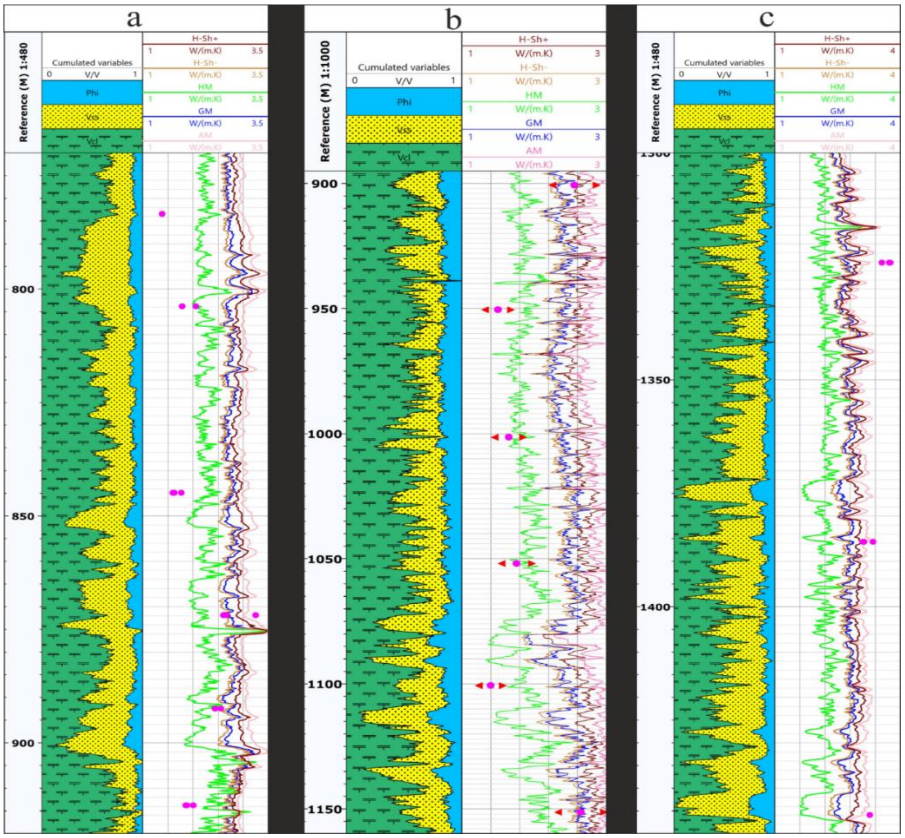

Figure 8

Bulk thermal conductivity values calculated by various mixing models: (a) and (b) represent the results of the Sz-2 and Mp-1 wells respectively, in case of intervals including clayey, marly,silty sections interbedded with fine grained sandstones contaminated with clay; (c) introduces the result of Sz-2 representing a section containing multiple sandstone interbeds. Purple circles are the measured thermal conductivites; in case of (b) red triangles define the error of laboratory measurements. Description of logs: dark red, H-Sh+: upper Hashin–Shtrikman bound, dark yellow, H-Sh-: lower Hashin–Shtrikman bound, green, HM: harmonic mean, dark blue, GM: geometric mean, pink, AM: arithmetic mean

Crossplots of each mixing models were created for better visualization *(Figure 9)*. The first noticeable phenomenon, also concluded by Hartmann et al. [9], is that in the case of an analogous mineral composition the geometric mean model closely follows the lower Hashin-Shtrikman bound, corresponding to a rock model representing spherical grains suspended in a fluid (*Figures 8, 9c* and *9d*). In case of pelitic samples, most of the mixing models overestimate the thermal conductivity based on laboratory measurements. Only the harmonic mean gives a better estimation *(Figure 9e)*, though this fit is also poor. All of the mixing models underestimate the psammitic samples and are incapable of giving higher thermal conductivity values than 4 W/(m*K), which can be explained with the low, 4.2 W/(m*K) matrix thermal conductivity. From these phenomena it is clearly visible that for better fit between the calculated and measured values, lower matrix thermal conductivity is needed for the pelite parameter and a higher value for the psammite.

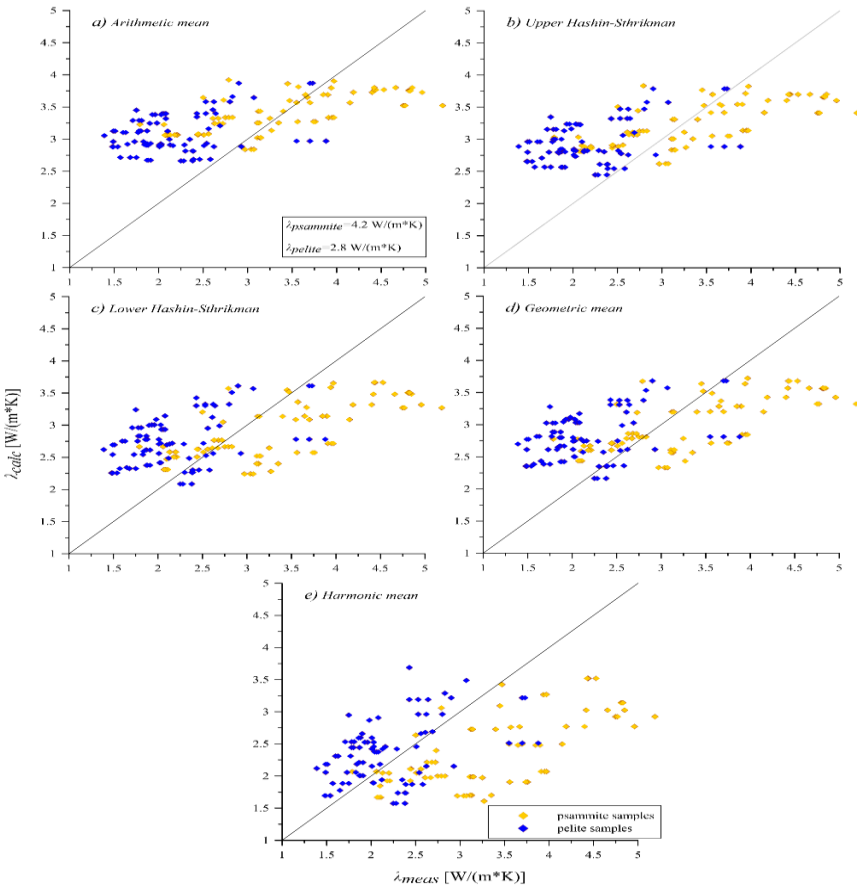

Figure 9

Crossplots of thermal conductivity values measured in laboratory and thermal conductivity values calculated by each mixing models using matrix thermal conductivities, after the work of Dövényi & Horváth [21]

3.2.2. Calculating new matrix thermal conductivities

The end-member thermal conductivities of Dövényi & Horváth [21] mentioned in Section 2.2.4 were used for this task with some modifications. An overview of the process can be seen in *Figure 10*. Thermal conductivities of laboratory measurements were used for the calculation and porosity values — extracted from our lithological inversion — were assigned to the samples. The porosity-thermal conductivity dataset was divided into two major groups: pelites and psammites. Evaluating the pelite and psammite end-member thermal conductivity as a first step, a weighted least squares inversion was applied using the standard deviations of laboratory measurements as weight factors. Two models were investigated: in the first model, the geometric mean was utilized as response function and in the second model the harmonic mean was employed. As a result, new matrix thermal conductivity values were evaluated. In case of both models a decrease in the pelite thermal conductivity and an increase in the psammite thermal conductivity could be observed, in line with our expectations *(Table 2)*.

Table 2

Result of the matrix thermal conductivity calculations

	Pelite	Psammite
Model 1	2.244 W/(m*K)	4.909 W/(m*K)
Model 2	2.616 W/(m*K)	6.667 W/(m*K)

In the second step, the mixing models detailed in Section 2.2 were recalculated for Model 1 and Model 2; thus, new crossplots were prepared as a final result (*Figures 11* & *12*). Crossplots of Model 1 can be seen in *Figure 11*. The first noticeable phenomenon — in comparison with results in *Figure 9* — is that the sets of points are less centralized in the middle section due to the higher psammite thermal conductivity value. In the case of Model 1 the geometric mean mixing model *(Figure 11d)* seems to be the best approximation for calculating the thermal conductivities, as the data points are located near the line of 45 degrees indicating the best fitting. In *Figure 12* the crossplots of Model 2 are represented. A much more scattered overall picture is visible compared to both *Figure 9* and *Figure 11*; however, the harmonic mean model seems to provide the most appropriate result when applying Model 2 *(Figure 12e)*. The geometric mean mixing model for Model 1 and the harmonic mean mixing model for Model 2 have given completely acceptable results for the two major groups (pelites and psammites). Examining the root-mean-square (RMS) values (standard deviation of the estimate) of the models given, no significant difference can be identified: 0.71 W/(m*K) for Model 1 with the geometric mean mixing model and 0.79 W/(m*K) for Model 2 with the harmonic mean mixing model. Therefore, it was necessary to test these models with a different method and choose the most reliable parameter set.

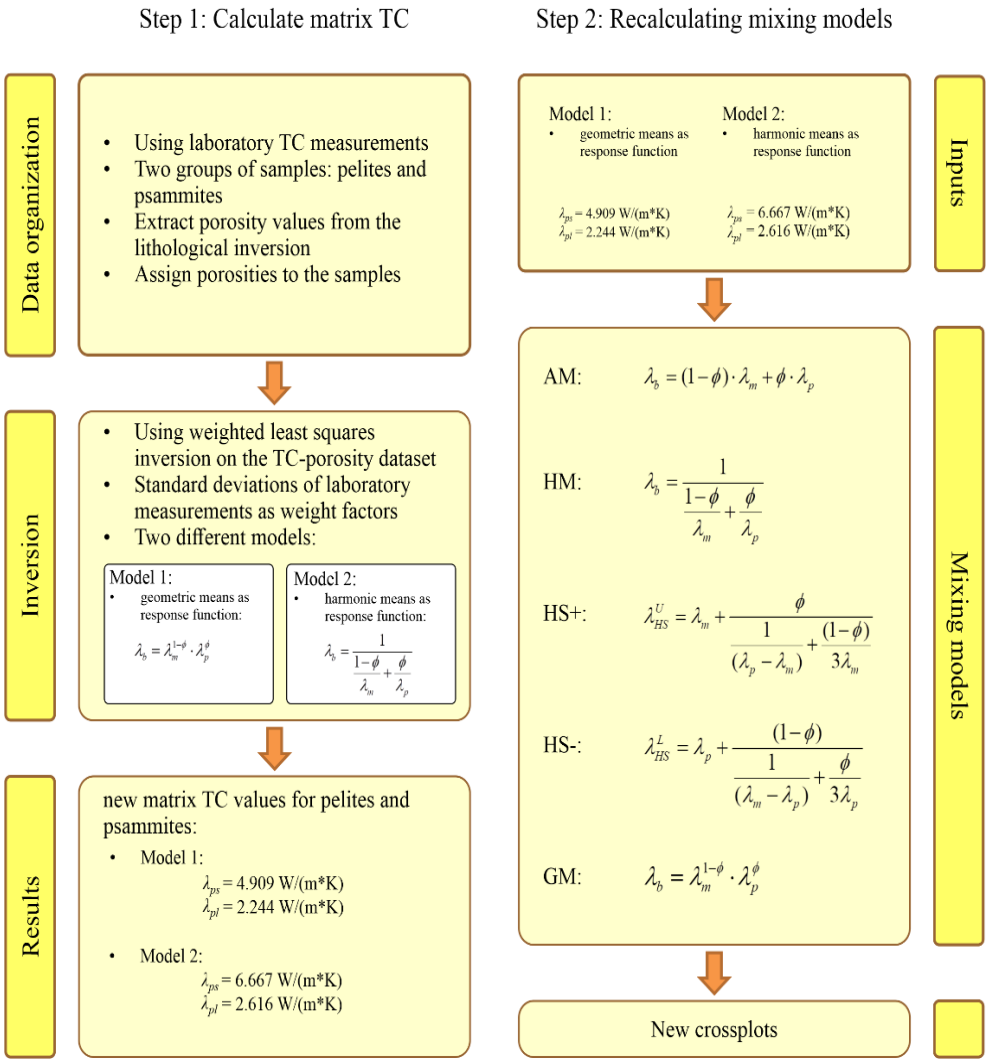

Figure 10

Flow chart of the process of calculating new matrix thermal conductivities (TC)

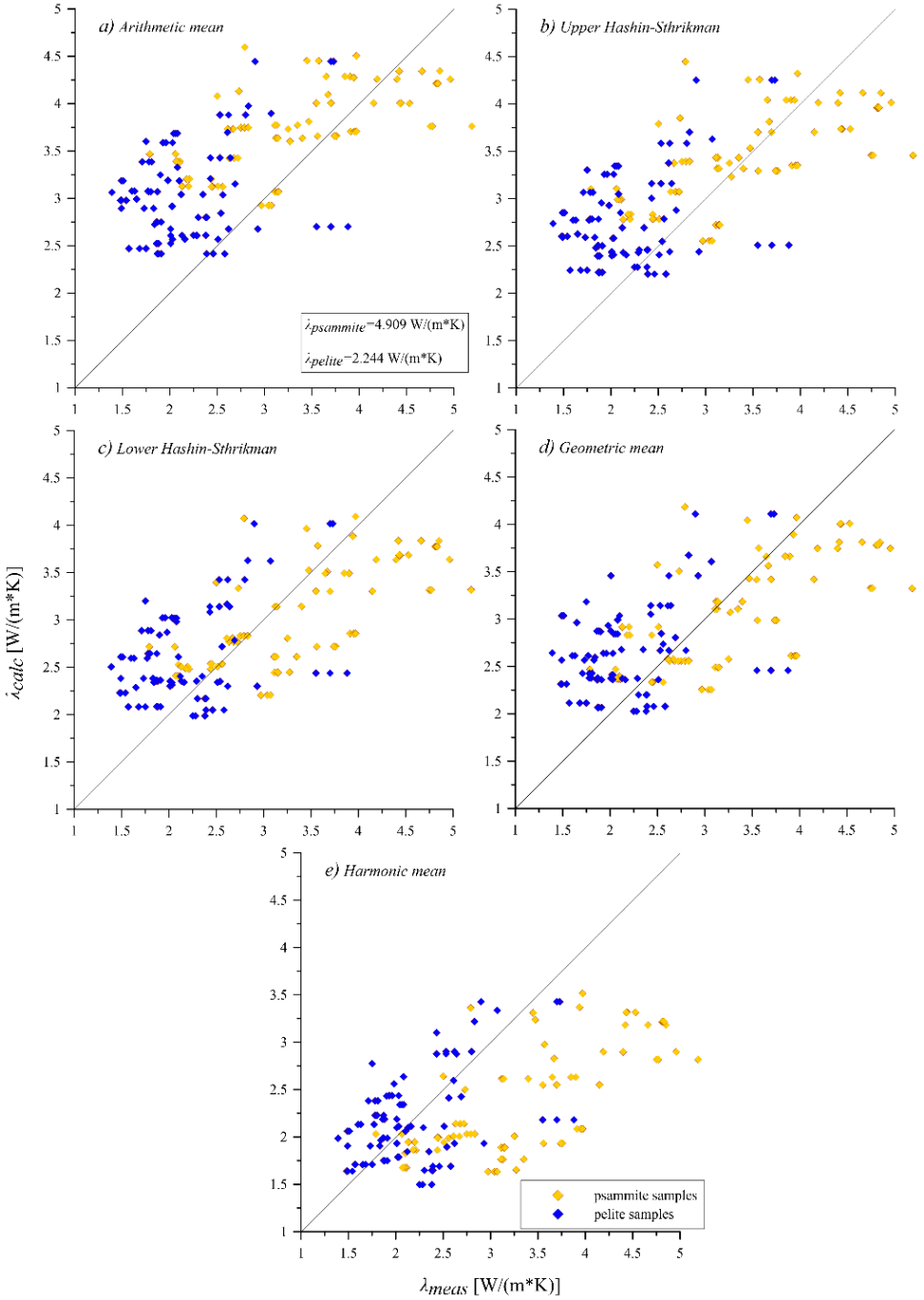

Figure 11

Crossplots of thermal conductivity values measured in the laboratory and thermal conductivity values calculated by each mixing models using Model 1 parameter set

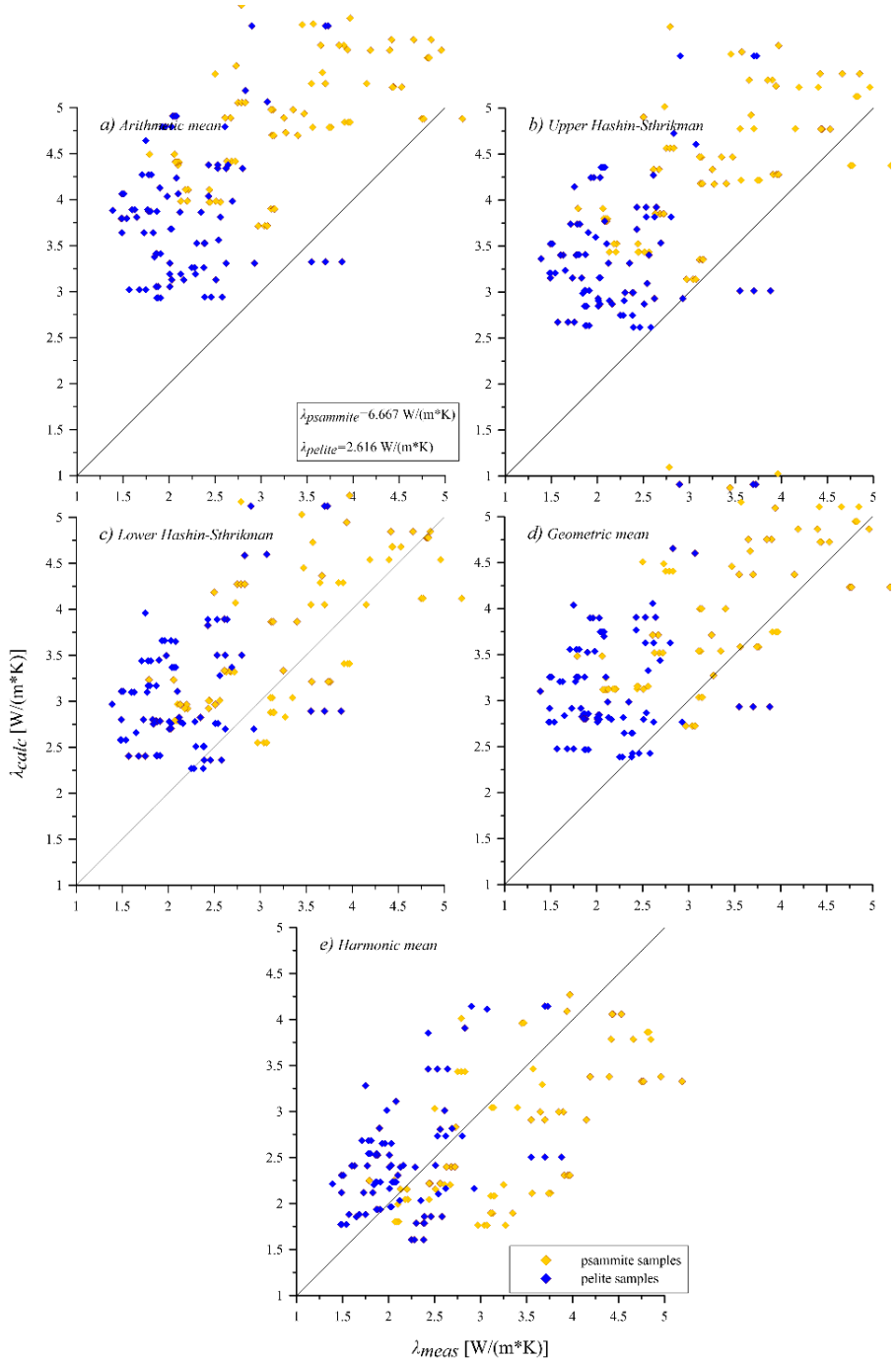

Figure 12

Crossplots of thermal conductivity values measured in laboratory and thermal conductivity values calculated by each mixing models using Model 2 parameter set

3.3. Temperature recalculation in the well Sz-2

The applicability of the results presented in the previous chapter was examined with the help of temperature measurements carried out in the well named Sz-2. The reason for selecting this particular well is that the most accurate temperature measurements were accomplished in it because the well had been in steady-state condition for two years before the measurements were carried out; therefore, the heat flow density, which is the basis of our methodology of testing, was determined with high precision ($q = 85 \pm 6.375$ mW/m^2). Assuming an isotropic, horizontally layered medium where the heat flows only in vertical direction, the following equation can be obtained for temperature:

$$T_i = T_{i-1} + \frac{q_s}{\lambda_i} \cdot \Delta z, \tag{13}$$

where q_s is the surface heat flow density [mW/m^2], T_i [°C] is the temperature, λ_i [W/(m*K)] is the thermal conductivity at ith depth, and Δz [m] is the depth increase. As the heat flow density is known ($q = 85 \pm 6.375$ mW/m^2), furthermore the thermal conductivity as a log is also known for both Model 1 and Model 2, it is feasible to recalculate the temperature in any particular depth point and compare it to the temperature value measured in the well. The results are shown in *Figure 13*. The purple dots indicate the temperature measurements, the lines mark the recalculated temperature logs in case of Model 1 (blue) and Model 2 (red) with a fixed heat flow density value. It is clearly noticeable that the temperature log using Model 2 parameter set follows the measured temperatures more precisely, meaning that the harmonic mean model seems to be the best approximation for determining thermal conductivity. Based on this result, Model 2 was used for redetermination of heat flow density in the studied wells.

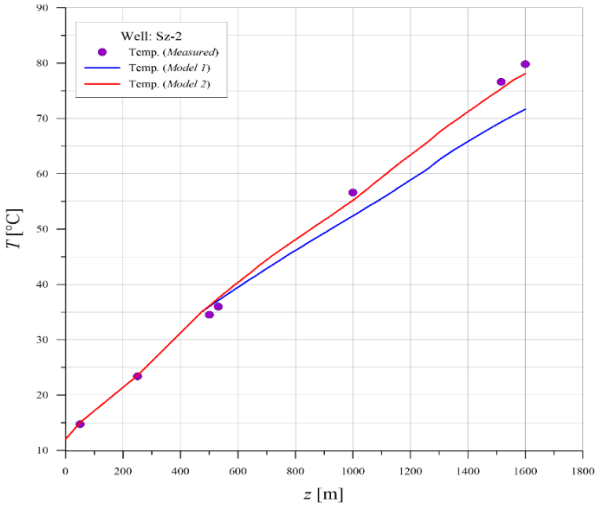

Figure 13

Recalculation of temperature in the Sz-2 well using Model 1 (blue line) and Model 2 (red line)

4. DISCUSSION

4.1. Thermal conductivity

A method was elaborated to calculate the thermal conductivity of Tertiary and Quaternary clastic sediments in Hungary taking into account 158 thermal conductivity measurements on core samples. After calculating the thermal conductivities using matrix parameters after the work of Dövényi & Horváth [21], it was clearly visible that the calibration was not satisfactory *(Figure 9)* and lower matrix thermal conductivity for the clay parameter and a higher value for the sand parameter were needed. With the new matrix thermal conductivity values a better result could be achieved.

4.2. Heat flow density

The heat flow density in the studied wells was determined by the Bullard plot presented in Section 2.3.1 in which the thermal conductivity values were calculated with Model 2 parameter set, as it was the best approximation. The temperature data were collected from the Geothermal Database of Hungary (GDH) [27] which contains more than 14,000 temperature data; furthermore, uncertainties were assigned for the temperature values based on the quality scale of GDH. The error propagation of heat flow densities was also estimated by the technique presented in Section 2.3.2. In *Figure 14* the studied wells are listed and the comparison between the heat flow density values from previous works (red points) [21, 28–31] and the values of our calculations (blue points) are shown. The black linesindicate the error bars of heat flow density values. It is clearly visible that our results are within the error range of the former heat flow density determinations, but our error values have decreased. Except for one well (named S-I), all recalculated heat flow densities are slightly higher but each value is within the bars of error found in the literature. For example in case of Well Sz-2 the previously determined 85 ± 6.375 mW/m^2 heat flow density has increased to 86.18 ± 2.84 mW/m^2. It can be said that the method established may be adequate to estimate the thermal conductivity in wells where no core sample was brought up. However, it should be mentioned that not only thermal conductivity plays an important role in properly estimating the heat flow density. The quality of temperature data and well logs also change from well to well, so these differences should be taken into consideration.

At this point our methodology has been successfully applied on 6 drilling wells. These wells were examined separately, but it is important to view our results on a larger scale. Figure 15 illustrates the heat flow density map of Hungary [32] and the locations of wells studied. Next to each well the recalculated heat flow density values are indicated with their error. It can be said that all heat flow densities fitting into the map on a regional scale, i.e. there is no contradiction between the map and our results.

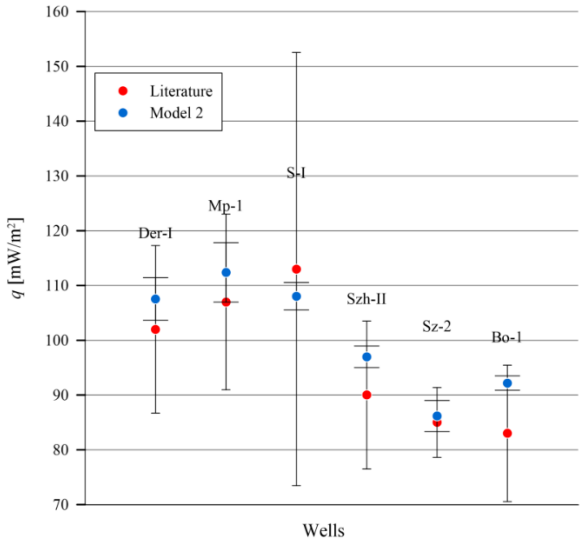

Figure 14
Comparison between the heat flow density values in different wells from previous works (red points) [21, 28–31] *and the values of our calculations (blue points) with error bars (black lines)*

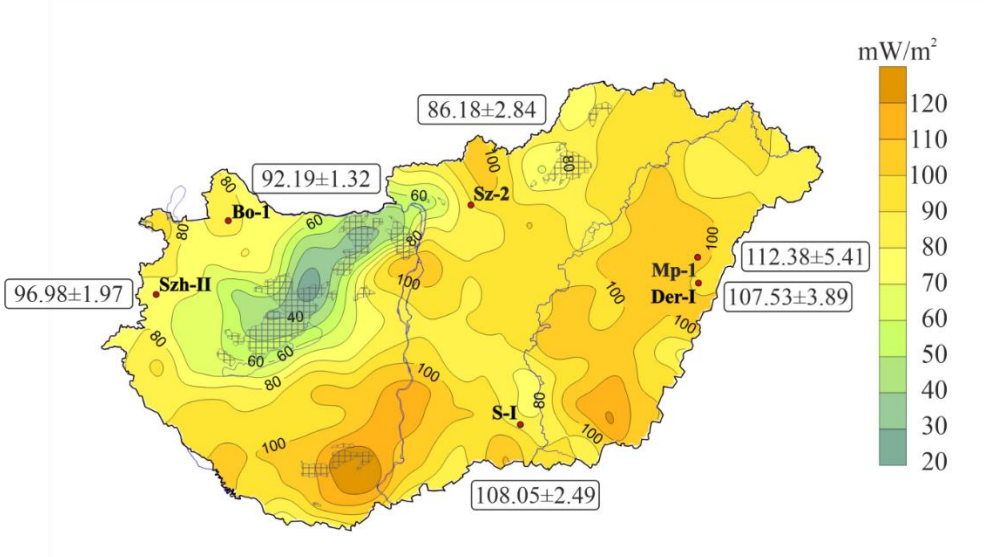

Figure 15
Heat flow density map of Hungary [32] *and the wells studied with the recalculated heat flow density values with their error*

5. CONCLUSIONS

After examining 6 drilling projects, our conclusion is that the thermal conductivity of clastic sediments in Hungary can be calculated by a harmonic mean model in which the volumetric fractions of clay, sand and water are present. This perception was tested by the temperature recalculation in the well named Sz-2.

A methodology was successfully elaborated for determining the thermal conductivity of clastic sediments using geophysical well logs and calculating the heat flow density and its error in a quality controlled way, which significantly increases the precision of the heat flow density calculation. With our method the error rate of the calculations of heat flow density has been successfully reduced. However, besides the thermal conductivity, the quality of temperature data and well logs play an important role in properly estimating the heat flow density.

ACKNOWLEDGEMENT

This work was supported by the Hungarian Scientific Research Fund (OTKA) in the framework of project No. K 129279. We are grateful to the Hungarian Oil Company (MOL Plc.) and institute of Mining and Geological Survey of Hungary for providing the well logs of boreholes.

REFERENCES

[1] Beck, A. E., Garven, G., Stegena, L. (1989). Hydrogeological Regimes and Their Subsurface Thermal Effects. *Geophysical Monograph*, 47 (2), AGU, IUGG, Washington DC, pp. 1–158.

[2] Lenkey, L., Dövényi, P., Horváth, F., Cloetingh, S. (2002): Geothermics of the Pannonian basin and its bearing on the neotectonics. In: Cloetingh, S., Horváth, F., Bada, G. and Lankreijer, A. (eds.). *Neotectonics and Surface Processes: the Pannonian Basin and Alpine/Carpathian System*. European Geosciences Union, Katlenburg-Lindau, Stephan Mueller Special Publication Series, vol. 3, pp. 29–40.

[3] Lipsey, L., Pluymaekers, M., Goldberg, T., van Oversteeg, K., Ghazaryan, L., Cloetingh, S., van Wees,, J.-D. (2016). Numerical modelling of thermal convection in the Luttelgeest carbonate platform, the Netherlands. *Geothermics*, 64, pp. 135–151.

[4] Schubert G., Turcotte D. L. (1982). *Geodynamics. Applications of Continuum Physics to Geological Problems.* John Wiley and Sons, New York.

[5] Cloetingh, S., van Wees, J. D., Ziegler, P. A., Lenkey, L., Beekman, F., Tesauro, M., Förster, A., Norden, B., Kaban, M., Hardebol, N., Bonté, D., Genter, A., Guillou-Frottier, L., Ter Voorde, M., Sokoutis, D., Willingshofer, E., Cornu, T., Wórum, G. (2010). Lithosphere tectonics and thermo-mechanical properties:

an integrated modelling approach for Enhanced Geothermal Systems exploration in Europe. *Earth-Science Reviews*, 102, pp. 159–206, DOI: 10.1016/j.earscirev.2010.05.003.

[6] Kilényi, É., Kröll, A., Obernauer, D., Šefara, J., Steinhauser, P., Szabó, Z., Wessely, G. (1991). Pre-Tertiary basement contour map of the Carpathian Basin beneath Austria, Czechoslovakia and Hungary. *Geophysical Transactions*, 36, pp.15–36.

[7] Brigaud, F., Chapman, D. S., Le Douaran, S. (1990). Estimating thermal conductivity in sedimentary basins using lithologic data and geophysical well logs. *The American Association of Petroleum Geologist Bulletin*, 74 (9), pp. 1459–1477.

[8] Demongodin, L., Pinoteau, B., Vasseur, G., Gable, R. (1991). Thermal conductivity and well logs: a case study in the Paris basin. *Geophysical Journal International*, 105 (3), pp. 675–691.

[9] Hartmann, A., Rath, V., Clauser, C. (2005). Thermal conductivity from core and well log data. *Internal Journal of Rock Mechanics & Mining Sciences*, 42 (7–8), pp. 1042–1055.

[10] Fuchs, S., Förster, A. (2013). Well-log based prediction of thermal conductivity of sedimentary successions: a case study from the North German Basin. *Geophysical Journal International*, 196 (1), pp. 291–311.

[11] Fuchs, S., Schütz, F., Förster, H. J., Förster, A. (2013). Evaluation of common mixing models for calculating bulk thermal conductivity of sedimentary rocks: correction charts and new conversion equations. *Geothermics*, 47, pp. 40–52.

[12] Hutt, J. R., Berg, J. W. (1968). Thermal and electrical conductivities of sandstone rocks and ocean sediments. *Geophysics*, 33 (3), pp. 489–500.

[13] Clauser, C. (2009). Heat Transport Processes in the Earth's Crust. *Surveys in Geophysics*, 30 (3), pp. 163–191.

[14] Popov, Y. A., Pribnow, D. F. C., Sass, J. H., Williams, C. F., Burkhardt, H. (1999): Characterization of rock thermal conductivity by high-resolution optical scanning. *Geothermics*, 28 (2), pp. 253–276.

[15] Dövényi, P., Horváth, F., Liebe, P., Gálfi, J., Erki, I. (1983): Geothermal Conditions of Hungary, *Geophysical Transactions*, 29 (1), pp. 3–114.

[16] Cull, J. P. (1974). Thermal conductivity probes for rapid measurements in rock. *Journal of Physics E: Scientific Instruments*, 7 (9), pp. 771–774.

[17] Szatmári, Z. (2010). *Mérések kiértékelése (Evaluating measurements)*. Lecture notes, Budapest University of Technology and Economics.

[18] Voigt, W. (1928). *Lehrbuch der Kristallphysik*. Teubner, Leipzig.

[19] Reuss, A. (1929). Berechnung der Fließgrenze von Mischkristallen auf Grund der Plastizitätsbedingung für Einkristalle. *Zeitschrift für Angewandte Mathematik und Mechanik*, 9 (1), pp. 49–58.

[20] Hashin, Z., Shtrikman, S. (1962). A variational approach to the theory of the effective magnetic permeability of multiphase materials. *Journal of Applied Physics*, 33 (10), pp. 3125–3131.

[21] Dövényi, P., Horváth, F. (1988). A review of temperature, thermal conductivity, and heat flow data from the Pannonian Basin. In: Royden, L. H., Horváth, F. (eds.). *The Pannonian Basin: A Study in Basin Evolution*. *AAPG Memoir 45*, American Association of Petroleum Geologists (AAPG), Tulsa, Oklahoma, pp. 195–233.

[22] Somerton, W. H. (1992). *Thermal Properties and Temperature-Related Behavior of Rock/Fluid Systems.* Amsterdam, Elsevier Science Publishers B.V., p. 258.

[23] York, D. (1966). Least-squares fitting of a straight line. *Canadian Journal of Physics.*, 44, pp. 1079–1086.

[24] York, D., Evensen, N. M., López Martinez, M., De Basabe Delgado, J. (2004). Unified equations for the slope, intercept, and standard errors of the best straight line. *American Journal of Physics*, 72 (3), pp. 367–375.

[25] Juhász, Gy. (1994). Comparison of the sedimentary sequences in Late Neogene subbasins in the Pannonian Basin, Hungary. *Földtani Közlöny*, 124 (4), pp. 341–365.

[26] Horváth, F., Musitz, B., Balázs, A., Végh, A., Uhrin, A., Nándor, A., Koroknai, B., Pap, N., Tóth, T., Wórum, G. (2015). Evolution of the Pannonian basin and its geothermal resources. *Geothermics*, 53, pp. 328–352.

[27] Dövényi, P. (1994). *Geophysical investigation of the lithosphere of the Pannonian basin.* PhD Thesis, Eötvös Loránd University, Budapest, pp. 127.

[28] Horváth, F., Dövényi, P., Erki, I., Liebe, P., Gálfi, J., Markó, L. (1981). *A Pannon medence geotermikus viszonyai.* Kutatási jelentés az MTA részére a 109/78-I. sz. megbízás alapján. ELTE Geofizikai Tanszék adattára, Budapest, pp. 1–100. (Geothermal conditions of the Pannonian basin. Research report for the Hungarian Academy of Sciences, Budapest.)

[29] Horváth, F., Erki, I., Dövényi, P. (1986). *Mikepércs-1. sz. fúrás geotermikus vizsgálata*. Kutatási jelentés a MÁFI megbízása alapján, ELTE, Budapest (kézirat). p. 21. (Geothermal investigation of well Mikepércs-1. Research report for the Hungarian Geological Institute, Budapest.)

[30] Horváth, F., Dövényi, P. (1987): A medencefejlődés modellezése. In: *GEOS GMK jelentése a KV megbízásából*. Budapest, pp. 476–672. (Modelling of basin evolution. Research report for the Hungarian Oil Research Company, Budapest.)

[31] Horváth, F., Dövényi, P., Erki, I., Lenkey, L. (1989). *A Szombathely-II sz, fúrás geotermikus vizsgálata*. Kutatási zárójelentés a MÁFI megbízásából, ELTE, Budapest, pp. 29. (Geothermal investigation of well Szombathelyy-II. Research report for the Hungarian Geological Institute, Budapest.)

[32] Lenkey, L., Mihályka, J., Paróczi, P. (in press). Review of geothermal conditions of Hungary. *Földtani Közlöny*.